Courant Institute of
Mathematical Sciences

AEC Computing and Applied Mathematics Center

Finite Difference Calculations for Hydrodynamic Flows Containing Discontinuities

Samuel Z. Burstein

New York University

AEC Computing and Applied Mathematics Center
Courant Institute of Mathematical Sciences
New York University

TID-4500   NYO-1480-33
43rd Ed.   MATHEMATICS

FINITE DIFFERENCE CALCULATIONS FOR

HYDRODYNAMIC FLOWS CONTAINING

DISCONTINUITIES

by

Samuel Z. Burstein

September 1965

Contract No. AT(30-1)-1480

FINITE DIFFERENCE CALCULATIONS FOR HYDRODYNAMIC
FLOWS CONTAINING DISCONTINUITIES

ABSTRACT

In this paper we show how to calculate the steady hypersonic inviscid flow, including a detached shock, around a blunt body. The steady flow is obtained as the limit for large time of time dependent flow, starting with plane flow impinging on the body. The transient flow is the solution of a mixed initial-boundary value problem for the partial differential equations of inviscid fluids which is solved by a difference scheme proposed by Lax and Wendroff. Our calculations show that by itself this difference scheme tends to be unstable and does not converge to the steady flow; by adding an artificial viscosity term we have succeeded in stabilizing the calculation. In Section 4 we give a fairly convincing theoretical explanation of this stabilizing effect and derive a new stability condition.

Both plane and cylindrical symmetries are considered; in the cylindrical case we use a variant of Richtmyer's twostep version of the Lax-Wendroff difference scheme. This method, as does Richtmyer's, requires much fewer arithmetic operations as compared to the one-step method.

TABLE OF CONTENTS

FINITE DIFFERENCE CALCULATIONS FOR HYDRODYNAMIC
FLOWS CONTAINING DISCONTINUITIES

Samuel Z. Burstein

1. Introduction

This report continues the exploration of certain explicit difference methods for fluid dynamic computations in three independent variables. The application of the Lax-Wendroff method was extended to a more difficult problem; the detached shock problem. The method of solution is to consider the problem to be of the mixed type, an initial and boundary value problem. By prescribing boundary conditions both on the body and at the upstream and downstream regions and by prescribing the initial data, a time-dependent solution was generated from the above conditions. Solutions for large times were obtained and these correspond to the steady state. Both plane and axisymmetric flows were considered and several difference methods were tested and compared.

In a previous paper [1] results were presented for a series of calculations relating to compressible flows in channels. These flows contain oblique shocks and for some shapes Mach reflections. It was noted that if Mach reflection took place, there were oscillations present in the downstream region of the flow field, i.e., behind the normal shock wave and extending to the boundary; no

such oscillations were detected for the case of regular reflection. It might be thought that the difference between the two cases can be tentatively explained as follows: the treatment of the downstream boundary by extrapolation introduced errors. In subsonic flow these errors propagate upstream and affect the accuracy of the solution but are swept out of the mesh in supersonic flows.

However severe difficulties were encountered in the numerical calculation of the detached shock problem. The solution of these difficulties shed light on the behavior of the difference equations and, in return, on the nature of the oscillations encountered in the Mach reflection calculation.

The author would like to acknowledge that during the course of this investigation he had many helpful discussions with Professor Peter Lax -- all of which made this work possible. I also thank Professor Robert Richtmyer for his comments on the paper.

2. Hydrodynamic differential equations

The conservation of mass, momentum and energy in inviscid time-dependent fluid motion are expressed by equations of divergence form

(2.1) $$\operatorname{div} \phi = 0 .$$

Here

(2.2) $$\phi = (w , f(w), g(w))$$

and div is the partial operator in three dimensional space-time

- 5 -

(2.3) $\qquad \text{div} = (\ )_{,t} + (\ )_{,x} + (\ )_{,y}$.

Hence

$$w_{,t} + f_{,x} + g_{,y} = 0 \ ;$$

w, f and g are vectors. The components of w are mass, momentum in the x- and y-direction and the total energy all per unit volume

$$w = \begin{pmatrix} \rho \\ \rho u \\ \rho v \\ E \end{pmatrix} .$$

The vectors f and g are non-linear vector valued functions corresponding to the fluxes in the x- and y-directions of the quantities w.

For the case of axially symmetric flows the equations of motion take the slightly different form,

(2.4) $\qquad \text{div } \phi = h$

where the vector $h = -\dfrac{v}{y}(w + \pi)$, $\pi^T = (0,0,0,p)$ and the coordinate y stands for the radial distance from the axis of symmetry. Equation (2.4) may be written in almost conservation form if the vector $\ell^T = (0,0,p,0)$ is introduced by

(2.5) $\qquad - yh + \begin{pmatrix} 0 \\ 0 \\ p \\ 0 \end{pmatrix} \equiv g$.

Expanding Eq. (2.4) by using the relations (2.2), (2.3), (2.4) and (2.5) yields

(2.6) $\qquad w,_t + f,_x + g,_y = -\ell .$

Thus the vector ϕ is replaced by $y\phi$ in Eq. (2.4) while the inhomogeneous term ℓ contains only one nonzero component in the radial momentum equation compared to four contained in h. For net points not on the axis of symmetry, Eq. (2.6) should be used for the generation of the difference scheme in axially symmetric flows.

The pressure p may be expressed in terms of the conservation variables and the ratio of specific heats of the gas, γ, through

(2.7) $\qquad p = (\gamma - 1)\ \{E - (m^2 + n^2)/2\rho\}$

where $m = \rho u$ and $n = \rho v$. With the use of Eq. (2.7), the vectors $f(w)$ and $g(w)$ become

$$f(w) = \begin{bmatrix} m \\ \dfrac{\gamma-3}{2}\dfrac{m^2}{\rho} + (\gamma-1)\{E- \dfrac{1}{2}\dfrac{n^2}{\rho}\} \\ \dfrac{mn}{\rho} \\ \dfrac{(1-\gamma)}{2}\ m\ (m^2 + n^2) + \gamma\ \dfrac{mE}{\rho} \end{bmatrix}$$

$$g(w) = \begin{bmatrix} n \\ \dfrac{nm}{\rho} \\ \dfrac{\gamma-3}{2}\dfrac{n^2}{\rho} + (\gamma-1)\{E- \dfrac{1}{2}\dfrac{m^2}{\rho}\} \\ \dfrac{1-\gamma}{2}\ n(n^2 + m^2) + \gamma\ \dfrac{nE}{\rho} \end{bmatrix}$$

For axially symmetric flows ρ is replaced by $y\rho$ everywhere in the above expressions.

3. Difference schemes of second order accuracy

The difference scheme that Lax and Wendroff used for one-dimensional calculations [3] and the two dimensional version which was analyzed in [2] is based on the Taylor expansion

$$(3.1) \quad w(t + \Delta t) = w(t) + \Delta t \; w,_t + \Delta t^2/2 \; w,_{tt} \; .$$

The error in the above expression is third order in the time interval Δt. The second term may be evaluated by substitution of the differential equation (2.3). If (2.3) is differentiated with respect to the independent variable time, then $-w,_{tt}$ is given by

$$(f,_x + g,_y),_t = (f,_t),_x + (g,_t),_y$$

$$(3.2) \qquad = (\tfrac{\partial f}{\partial w} \; w,_t),_x + (\tfrac{\partial g}{\partial w} \; w,_t),_y$$

$$\equiv [A(f,_x + g,_y)],_x + [B(f,_x + g,_y)],_y \; .$$

In (3.2) the matrices A and B are the Jacobians $f,_w$ and $g,_w$ respectively and are given by

$$A(w) = - \begin{bmatrix} 0 & -1 & 0 & 0 \\ \frac{3-\gamma}{2}X^2 + \frac{1-\gamma}{2}Y^2 & (\gamma-3)X & (\gamma-1)Y & (1-\gamma) \\ XY & -Y & -X & 0 \\ \gamma XZ + (1-\gamma)X(X^2+Y^2) & -\gamma Z + \frac{\gamma-1}{2}(3X^2+Y^2) & (\gamma-1)XY & -\gamma X \end{bmatrix}$$

(3.3)

$$B(w) = - \begin{bmatrix} 0 & 0 & -1 & 0 \\ XY & -Y & -X & 0 \\ \frac{3-\gamma}{2}Y^2 + \frac{1-\gamma}{2}X^2 & (\gamma-1)X & (\gamma-3)Y & (1-\gamma) \\ \gamma YZ + (1-\gamma)Y(X^2+Y^2) & (\gamma-1)XY & -\gamma Z + \frac{\gamma-1}{2}(3Y^2+X^2) & -\gamma Y \end{bmatrix}$$

The abbreviations

$$X = m/\rho \; , \quad Y = n/\rho \; , \quad Z = E/\rho$$

have been used.

Equations (2.3) and (3.2) when substituted into (3.1) yield

$$w(t + \Delta t) = w(t) + \Delta t(f,_x + g,_y) +$$

(3.3')

$$+ \frac{\Delta t^2}{2}\{[A(f,_x+g,_y)],_x + [B(f,_x+g,_y)],_y\}.$$

To preserve the high order accuracy the terms containing first derivatives must be approximated by centered differences while the term containing the second derivatives, since it is O (Δt^2), may be approximated by uncentered differences. However, to center the entire expression consider the vectors C evaluated at the half interval (see Fig. 1a):

$$C(\Delta X/2) = \frac{f(x^+,y)+f(x,y)}{2} + \frac{\lambda}{4}(A^++A)\{f(x^+,y)-f(x,y)+$$

(3.4a)

$$+ \frac{1}{4}[g(x^+,y^+)+g(x,y^+) - g(x^+,y^-)-g(x,y^-)]\} .$$

To form $C(-\Delta X/2)$, we wish to translate the argument X by the amount $-\Delta X$. Multiplication by the translation operator T gives

(3.4b)
$$C(-\Delta X/2) = T_{-1}^{(X)} C(\Delta X/2) .$$

Similarly in the y direction

$$C(\Delta Y/2) = \frac{g(x,y^+)+g(x,y)}{2} + \frac{\lambda}{4}(B^++B)\{\frac{1}{4}[f(x^+,y^+)+$$

(3.4c)

$$+ f(x^+,y)-f(x^+,y^-)-f(x,y^-)]+g(x,y^+)-g(x,y)\},$$

and

(3.4d)
$$C(-\Delta Y/2) = T_{-1}^{(Y)} C(\Delta Y/2) .$$

We have used the notation $A^+ = A(X+\Delta X)$, $B^+ = B(Y+\Delta Y)$, etc. Then the difference approximation to Eq. (2.1) is

(3.5) $w(t+\Delta t) = w(t)+\lambda\{[C(\Delta X/2)-C(-\Delta X/2)]+[C(\Delta Y/2)-C(-\Delta Y/2)]\}.$

Here $\lambda = \Delta t/\Delta$ where $\Delta = \Delta x = \Delta y$. It is seen then, that by
centering the difference scheme has one of the properties
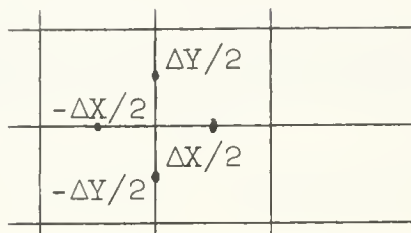of the differential equation; it is in divergence free form.

Figure la

The solution of the axially symmetric equations can
be achieved more simply by a two step calculation analogous
to the one developed by R. Richtmyer [4]. Two step methods
have the advantage of not requiring the computation of the
matrices A and B and hence matrix-vector multiplication
are eliminated. A variant of the two step Lax-Wendroff
scheme in two dimensions is:

<u>Step 1</u>: generates temporary data at the four points (•)
($k = i \pm 1/2$, $\ell = j \pm 1/2$, $t + \Delta t$) by the nine points (x)
shown in Fig. lb.

$$w_{k,\ell}(t+\Delta t) = \frac{1}{4}\left(w_{k+\frac{1}{2},\ell+\frac{1}{2}} + w_{k+\frac{1}{2},\ell-\frac{1}{2}} + w_{k-\frac{1}{2},\ell+\frac{1}{2}} \right.$$

$$\left. + w_{k-\frac{1}{2},\ell-\frac{1}{2}}\right) + \frac{\lambda}{2}\left\{f_{k+\frac{1}{2},\ell+\frac{1}{2}} - f_{k-\frac{1}{2},\ell+\frac{1}{2}} \right.$$

(3.6)

$$+ f_{k+\frac{1}{2},\ell-\frac{1}{2}} - f_{k-\frac{1}{2},\ell-\frac{1}{2}}) + \frac{\lambda}{2}\{g_{k+\frac{1}{2},\ell+\frac{1}{2}} - g_{k+\frac{1}{2},\ell-\frac{1}{2}} +$$

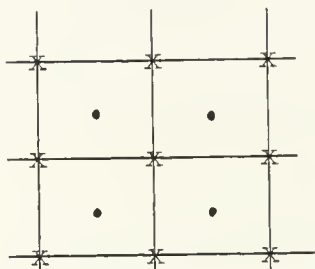$$+ g_{k-\frac{1}{2},\ell+\frac{1}{2}} - g_{k-\frac{1}{2},\ell-\frac{1}{2}}) \ .$$

Figure 1b

<u>Step 2</u>:

$$w_{i,j}(t+\Delta t) = w_{i,j}(t) + \frac{\lambda}{4}(f_{i+1,j} - f_{i-1,j} + f_{\hat{x}}^{t+\Delta t}) +$$

(3.7)

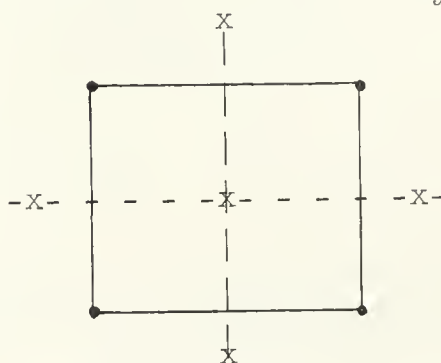$$+ \frac{\lambda}{4}(g_{i,j+1} - g_{i,j-1} + g_{\hat{y}}^{t+\Delta t}) \ .$$

Figure 1b'

The notation $f_{\hat{x}}^{t+\Delta t}$ expresses the fact that the x-centered

difference in f obtained at time t + Δt should be evaluated

from the formula:

$$f_{\hat{x}}^{t+\Delta t} = f(w_{i+\frac{1}{2},j+\frac{1}{2}}) - f(w_{i-\frac{1}{2},j+\frac{1}{2}}) + f(w_{i+\frac{1}{2},j-\frac{1}{2}}) -$$

$$- f(w_{i-\frac{1}{2},j-\frac{1}{2}})$$

and similarly for $g_{\hat{y}}^{t+\Delta t}$. Fig. (1b') shows as solid lines difference approximations to $f,_x$ and $g,_y$ at $t+\Delta t$ while the dashed lines are approximations at t. The one dimensional version of this scheme was originally suggested by B. Wendroff. The method centers all quantities at the point $(i,j,t+\Delta t/2)$ by the averaging procedure contained in Eq. (3.7), just as is done by the method of Taylor expansion in Eq. (3.1).

For axially-symmetric flows difference equations (3.6) and (3.7) are modified slightly. By inserting the terms

(3.6a) $\quad \frac{\Delta t}{4} (\ell_{k+\frac{1}{2},\ell+\frac{1}{2}}^{+\ell}{}_{k+\frac{1}{2},\ell-\frac{1}{2}}^{+\ell}{}_{k-\frac{1}{2},\ell+\frac{1}{2}}^{+\ell}{}_{k-\frac{1}{2},\ell-\frac{1}{2}})$

on the right hand side of Eq. (3.6) and

(3.7a) $\quad \frac{\Delta t}{2} [\ell_{i,j}(t)+\ell_{k,\ell}(t+\Delta t)], \; \ell_{k,\ell}(t+\Delta t)= \frac{1}{4}(\ell_{i\pm\frac{1}{2},j\pm\frac{1}{2}})^{t+\Delta t}$

on the right hand side of Eq. (3.7), the two step method can be used for axially symmetric flows. Equations (3.6a) and (3.7a) center the inhomogeneous term at point $(i,j, t+\frac{1}{2}\Delta t)$ consistent with the other terms in Eqs. (3.6) and (3.7).

Equations (3.6) and (3.7) may be linearized by allowing

f = Aw and g = Bw where A and B are considered constant. Then, combining equations (3.6) and (3.7) and substituting $w(\ell\Delta x, m\Delta y) = w^0 e^{i(k_x\ell\Delta x + k_y m\Delta y)}$, one obtains the amplification matrix [5]

$$G' = I + iA\lambda\{\tfrac{3}{4}\sin\xi + \tfrac{1}{4}\sin\xi\cos\eta\} + iB\lambda\{\tfrac{3}{4}\sin\eta +$$

(3.8)
$$+ \tfrac{1}{4}\sin\eta\cos\xi\} + \frac{A^2\lambda^2}{2}(\cos\xi - 1)(1 + \cos\eta) +$$

$$+ \frac{B^2\lambda^2}{2}(\cos\eta - 1)(1 + \cos\xi) - \frac{AB + BA}{2}\lambda^2\sin\xi\sin\eta ,$$

where $\xi = k_x\Delta x$, $\eta = k_y\Delta y$ and $\lambda = \Delta t/\Delta x$.

It may be verified that (3.8) can be written as

$$G' = I + i\lambda\{A\sin\xi(\frac{3 + \cos\eta}{4}) + B\sin\eta(\frac{3 + \cos\xi}{4})\}$$

(3.9)
$$- \frac{\lambda^2}{2}\{A\sqrt{(1 - \cos\xi)(1 + \cos\eta)} + B\sqrt{(1 - \cos\eta)(1 + \cos\xi)}\}^2 .$$

For $\xi, \eta \ll 1$ the approximations

$$\sin\xi = \xi , \quad 1 - \cos\xi = -\xi^2/2 , \quad 1 + \cos\xi = 2 - \xi^2/2 ,$$

may be used. Equation (3.9) becomes

$$G' = I + i\lambda(A\xi + B\eta) - \frac{\lambda^2}{2}(A\xi + B\eta)^2 + \mathcal{O}(\xi^3, \eta^3) .$$

Then, modulo terms of third order in ξ and η,

$$G' = e^{i\lambda(A\xi + B\eta)} .$$

This is the exact amplification matrix of the differential equation $w_t + Aw_x + Bw_y$. Hence it is clear that the set of

- 14 -

equations (3.6) and (3.7) are second order accurate.

4. A non-linear instability

In a recent paper Lax and Wendroff presented a stability proof of the second order difference method given by Eq. (3.5). We call the amplification matrix associated with the linearized form of Eq. (3.5) G; it is given by

$$G(\xi,\eta) = I + i (A \sin \xi + B \sin \eta) - A^2(1-\cos \xi) -$$
(4.1)
$$- B^2(1-\cos \eta) - (\frac{AB + BA}{2}) \sin \xi \sin \eta .$$

In order to prove stability one has to show that all eigenvalues of the amplification matrix are ≤ 1 in absolute value (von Neumann condition); this follows if the inner product

(4.1)'
$$(Gq , q) \leq 1$$

for all unit vectors q. In fact (4.1)' implies that $|G^n| \leq K$ for integer powers of n, i.e., n = 1,2,... . The difference scheme associated with G will be stable, at least if the coefficients of G are constant,[*] since

[*]Recently, Lax and Nirenberg have shown how to extend this conclusion to G with variable coefficients.

the solutions of the difference scheme (obtained by n successive multiplications of the difference operator) will be bounded. This is a consequence of the isometry of the L_2 norm when a fourier transform is made on the linear difference operator to obtain the amplification matrix. An analysis presented in [2] gives the following inequality:

$$|(Gq , q)|^2 \leq 1 - |Aq|^2(1- 8|Aq|^2)(1-\cos \xi)^2 -$$

(4.2)

$$- |Bq|^2(1- 8|Bq|^2)(1-\cos \eta)^2 .$$

This expression is less than unity if the requirements

$$A^2 \leq 1/8 , \qquad B^2 \leq 1/8 ,$$

are satisfied. For the case of equal spatial stepsize $\Delta x = \Delta y = \Delta$ this condition can be expressed as

$$(4.3) \qquad \frac{\Delta t}{\Delta} \leq \frac{1}{\sigma^* \sqrt{8}} , \qquad \sigma^* = \text{max eigvalue of A or B.}$$

In [1] is was shown empirically that the above stability condition is too stringent; it can be exceeded in practical applications without causing instability; in particular $\Delta t/\Delta = 1/\sqrt{2}\sigma^*$, which is twice as large as permitted by (4.3) yielded stable results. It was even possible to go slightly ($\approx 10\%$) beyond this numerical estimate. However, for the class of problems considered in this paper, even satisfying 1/10 of condition (4.3) led to numerical

instability during the early transient portion of the
flow (pointwise values of the density ρ and energy E.
> $10^3 \sim 10^5$ after which the density became negative).
During this time, the shock, having been produced
impulsively at the face of the body, was in the process
of detaching itself; instabilities were observed in
two regions: within the shock close to the axis of
symmetry and at the corner of the body. The corner
problem could be removed if a first order difference
approximation (discussed in Section 7) was used on the
top of the body. But within the shock negative
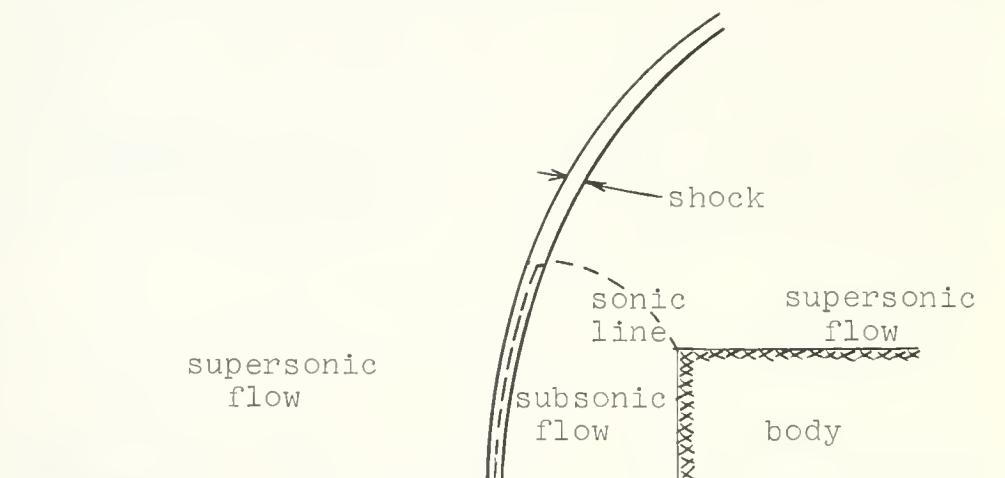densities were still obtained.

Figure 1c

Figure 2 shows schematically the growth of the
solution, at the shock, when an instability is present.
The highly oscillatory nature of the solution will grow
in time if the calculation is allowed to continue. The

data given in Figures 2 and 3 were obtained from results
which were an attempt to eliminate the early instability
(after approximately 60 cycles) that was obtained with
Eq. (3.5). Here, a modification in the coefficient of
the second term [5] in (3.4a), $\lambda/4(A^{+}+A)\cdot D$ and (3.4c),
$\lambda/4(B^{+}+B)\cdot D$ where $D > 1$ allowed the calculation to be
carried out as far as 500 cycles but eventually the
phenomenon shown in Figure 2 resulted. For $D > 1$, the
accuracy of the difference scheme is no longer second
order. The result of a case for $D = 3$ is given in
Figure 3 which shows the shock position for successive
times. At the point where the shock position becomes
stationary (at approximately 490 cycles), however,
instability results. The growth of the amplitude of
short wave length components of the solution for density
ρ, is shown in Figure 2. This was localized near the
axis of symmetry at the shock.

The fourth order artificial viscosity term which is
discussed in [2] was also tested with Eq. (3.5). It had
virtually no effect on the stability of the numerical
results.

These results were surprising but can be explained
by the following argument. Inequality (4.2) together with
the stability condition show that the eigenvalues of G are,
for $\xi, \eta \neq 0$, definitely less than one; this means that high
amplitude waves are damped. However, if $|Aq|$ or $|Bq|$ happen

to be zero, this damping is absent. Now $|Aq|$, $|Bq|$ can vanish if and only if zero is an eigenvalue of A or B. The eigenvalues of A, B are $u \pm c,u$ and $v \pm c,v$. Hence for points, lines or surfaces in the flow where

Condition I: $u/c = 1$, or $v/c = 1$,

(c is the local sound speed) or

Condition II: $u = 0 = v$,

one of the eigenvalues becomes zero. Condition I corresponds to local one dimensional sonic flow while condition II corresponds to flow at stagnation points. If the sonic line is extended, it will pass within the shock (see Fig. 1c) so that near the axis of symmetry since the flow is locally one-dimensional, $\eta = 0$, Condition I occurs; i.e., there will be no damping for the associated linear difference scheme (4.2) and hence $|(Gq , q)|^2 = 1$. Since this condition of neutral stability occurs in a part of the flow where the basis of applying linear analyses are weakest, (where flow properties vary most rapidly) a nonlinear statement of stability is suspect. Such second order schemes (including the two step method given by Eqs. (3.6) and (3.7)) will probably need additional damping terms for successful results. These terms must be third order so as to preserve the numerical accuracy.

$$(5.3a) \quad \alpha_i = \frac{1}{2} \kappa_i \frac{|\sigma_i(\omega) - \sigma_i(\omega')|}{(\bar{\sigma}_i - \bar{\sigma}_j)(\bar{\sigma}_i - \bar{\sigma}_k)} , \quad i = 1, 2, 3, \quad j \neq i, \quad k \neq i, j.$$

Here the barred quantities are understood to be averages over the interval (ω, ω'), and κ_i may be a function of σ or constant. This will insure that if the flow is locally constant the α_i will vanish. A similar relationship can be written for β_i in terms of $\sigma(B)$. With this choice for α and β, the coefficients of Eq. (5.2) can be put in the form

$$a_0 = \sum_{\substack{i=1, j \neq i \\ k \neq i, j}}^{3} \alpha_i \sigma_j \sigma_k ,$$

$$(5.3b) \qquad a_1 = - \sum_{\substack{i=1, j \neq i \\ k \neq i, j}}^{3} \alpha_i (\sigma_j + \sigma_k) ,$$

$$a_2 = \sum_{i=1}^{3} \alpha_i .$$

Then the matrices defined in (5.2) can be given by

$$Q^X = \sum_{\substack{i=1, j \neq i \\ k \neq i, j}}^{3} \alpha_i \{ (\bar{A} - \bar{\sigma}_j I)(\bar{A} - \bar{\sigma}_k I) ,$$

$$(5.4)$$

$$Q^y = \sum_{\substack{i=1, j \neq i \\ k \neq i, j}}^{3} \beta_i (\bar{B} - \bar{\sigma}_j I)(\bar{B} - \bar{\sigma}_k I) \} .$$

It is clear that with such a choice of coefficients the

eigenvalues of Q^x or Q^y will be proportional to the
difference of the eigenvalues of A or B in the interval
(ω, ω'), i.e.

$$Q = \frac{1}{2} \kappa_i |\sigma_i(\omega) - \sigma_i(\omega')| \cdot I .$$

Hence since there will always be at least one non-zero
eigenvalue, the viscosity will contribute to the solution
in regions where the solution varies most rapidly. This
will insure us that the difference scheme will have
dissipation.

Hence the complete difference scheme obtained by
combining Eq. (3.5) with the artificial viscosity given
by Eq. (5.1) is

$$w(t+\Delta t) = w(t) + \lambda\{D_x[L_x C(x) + \frac{1}{2} Q^x D_x' w] +$$

(5.5)

$$+ D_y[L_y C(y) + \frac{1}{2} Q^y D_y' w]\} .$$

We have used $L_x C(x) = \frac{1}{2} \{C(x+\Delta x)+C(x)\} = C(\Delta x/2)$ as the
forward averaging operator, D_x and D_x' as the centered and
forward difference operators respectively.

For the Lagrangian system of hydrodynamic equations
these coefficients reduce to that given by Lax and
Wendroff i.e.,

$$a_0 = 0 = a_1 ,$$

$$a_2 = \frac{1}{2} \kappa \frac{|c(\omega)-c(\omega')|}{\bar{c}^2} .$$

In the next section we use this Lagrangian form of
the viscosity to show stability of the Lax-Wendroff
scheme with the added artificial viscosity.

6. Stability analysis of second order scheme with viscosity

In order to study the stability of the difference
schemes we first linearize the equations by taking the
matrices A and B to be locally constant. We assume that
the real matrices A, B are symmetric or at least they can
be symmetrized by a similarity transformation. Also, for
simplicity, let $\Delta x = \Delta y = \Delta t = 1$. We also take the
viscosity to be of the form

$$(6.1) \qquad Q(A,B) = Q^x(A) + Q^y(B) = \frac{1}{2}\alpha A^2 + \frac{1}{2}\beta B^2 ,$$

where α and β are constant. This choice of Q is then
substituted into (5.1) and the result is linearized,
i.e. $\frac{1}{2}\alpha A^2 D_x^2 w + \frac{1}{2}\beta B^2 D_y^2 w$, where the second difference
operator is represented by D^2. Take the Fourier transform
of the above and add it to the amplification matris given
by Eq. (4.1); the result is:

$$G(\xi,\eta) = I + i(A \sin \xi + B \sin \eta) - (1 + \frac{1}{2}\alpha)A^2(1-\cos \xi)$$
$$(6.2)$$
$$- (1 + \frac{1}{2}\beta)B^2(1 - \cos \eta) - \frac{AB + BA}{2} \sin \xi \sin \eta .$$

The proof basically parallels that presented by Lax and
Wendroff [2]; we give all steps for completeness.

We wish to estimate the quantity (Gq, q) for all unit vectors q. G is separated into its real and imaginary parts

$$G = X + iY$$

where

$$Y = A \sin \xi + B \sin \eta$$

and

$$X = I - R$$

with

$$(6.3) \quad R = (1 + \frac{1}{2}\alpha)A^2\Theta + (1 + \frac{1}{2}\beta)B^2\Phi + \frac{AB + BA}{2} \sin \xi \sin \eta.$$

We have used the definitions $\Theta = 1 - \cos \xi$ and $\Phi = 1 - \cos \eta$. Now

$$(Gq, q) = (Xq, q) + i(Yq, q).$$

Since A and B are real and symmetric, it follows that X and Y are real and symmetric; hence

$$(6.4) \quad |(Gq, q)|^2 = (Xq, q)^2 + (Yq, q)^2.$$

R can be given by the identity

$$(6.5) \quad R \equiv \frac{1}{2}A^2\Theta^2 + \frac{1}{2}B^2\Phi^2 + \frac{1}{2}Y^2 + \frac{1}{2}\alpha A^2\Theta + \frac{1}{2}\beta B^2\Phi.$$

The proof proceeds by computing the right hand side of Eq. (6.4). Using the abbreviations $x = (Xq, q)$, $y = (Yq, q)$, and $r = (Rq, q)$ the absolute value of the real part of the inner product of the amplification matrix is

$$(6.6) \qquad x^2 = (1-r)^2 = 1 - 2r - r^2 .$$

Now the identity in R, Eq. (6.5), is used to obtain the
second term in Eq. (6.6) while the definition of R, given
by Eq. (6.3), is used for the evaluation of r^2. Taking
the inner product of Eq. (6.5) and using the Schwartz
inequality $(Yq^2 ,q) = |Yq|^2 \geq y^2$, we obtain

$$(6.7) \quad r \leq \tfrac{1}{2} A^2 \Theta^2 + \tfrac{1}{2} B^2 \Phi^2 + \tfrac{1}{2} y^2 + \tfrac{1}{2} \alpha A^2 \Theta + \tfrac{1}{2} \beta B^2 \Phi .$$

To obtain $|(Rq ,q)|^2$, multiply Eq. (6.3) by q and form
the inner product. One of the resulting terms,
$Re(Aq , Bq) \sin\xi \sin\eta$, may be estimated by the Schwartz
inequality

$$\leq |Aq| \, |\sin\xi| \, |Bq| \, |\sin\eta| \leq \{ |Aq|^2 \Theta + |Bq|^2 \Phi \} .$$

The trigonometric inequalities $\Theta \geq \tfrac{1}{2} \sin^2 \xi$ and
$\Phi \geq \tfrac{1}{2} \sin^2 \phi$ have been used. Using this result, Eq. (6.7)
becomes

$$r \leq |Aq|^2 (2 + \tfrac{1}{2}\alpha)\Theta + |Bq|^2 (2 + \tfrac{1}{2}\beta)\Phi$$

or

$$r^2 \leq (|Aq|^2)^2 \; \Theta^2 \{ (2+\tfrac{\alpha}{2})^2 + (2+\tfrac{\alpha}{2})(2+\tfrac{\beta}{2}) \}$$

$$(6.8)$$

$$+ (|Bq|^2)^2 \Phi \{ (2+\tfrac{\beta}{2})^2 + (2+\tfrac{\beta}{2})(2+\tfrac{\alpha}{2}) \} .$$

Substituting Eqs. (6.8) and (6.7) into Eq. (6.6) gives

$$x^2 + y^2 \leq 1 - |Aq|^2\{(1+\alpha) - \alpha^1|Aq|^2\}\widehat{\Theta}^2 -$$

(6.9)
$$- |Bq|^2\{(1+\beta) - \beta^1|Bq|^2\}\overline{\Phi}^2 .$$

We have used the trigonometric inequalities (for $\xi, \eta \sim \pi$) $\widehat{\Theta}^2 \geq \widehat{\Theta}$ and $\overline{\Phi}^2 \geq \overline{\Phi}$ (Short wave length disturbances must be damped so that their growth will not affect the numerical solution; see Figure 2) to obtain Eq. (6.9). The right hand side is less than one if

(6.10) $\quad |Aq|^2 = |\sigma(A)q|^2 \leq \dfrac{1+\alpha}{\alpha^1} ; \quad |Bq|^2 = |\sigma(B)q|^2 \leq \dfrac{1+\beta}{\beta^1} .$

α^1 and β^1 are abbreviations for the quantities in brackets in Eq. (6.8).

It is interesting to note that Eq. (6.9) is of the same form as Eq. (4.2). The argument presented in Section 4 on nonlinear stability would appear to hold in the present case. It must be concluded (in light of the numerical experiments performed with Eq. (5.5)) that linearization eliminates many important features of the difference scheme, e.g. nonlinear terms (see Richtmyer and Morton [7]). For the simple case of equal coefficients for the viscosity, Eq. (6.10) becomes

$$\sigma^2(A) \leq \frac{1+\alpha}{2(2+\frac{\alpha}{2})^2} = f(\alpha) .$$

The max of $f(\alpha)$ is for $\alpha = 2$, $f(2) = 1/6$. Hence there is hope that the scheme will be stable for

(6.11)
$$\frac{\Delta t}{\Delta x} \, |\sigma(A)| \leq \frac{1}{\sqrt{6}} \quad ,$$

while a similar expression holds for $\sigma(B)$. This is somewhat larger than the value $1/\sqrt{8}$ $(\alpha = 0)$, Lax and Wendroff obtained.[*] The term given by Eqs. (5.1) and (6.1) which is an artificial viscosity, clearly has a stabilizing influence on the difference scheme Eq. (3.5), since the allowable time increment is larger. Similar results hold for the more complicated forms of viscosity used in the numerical calculation, i.e. Eqs. (5.1) and (5.2).

The test of the stability condition was made using a constant to represent the right hand side of (6.11). This numerical value was fed into the machine via a data card and the resulting solution was checked every 30 cycles of computation. No other changes were made and the results appear in Table 1. The theoretical limit $r < .408$ (which is close to the Lax Wendroff value of .354) agrees within the accuracy obtained with the numerical estimate of Table 1. Additional experiments will be performed, especially for the case of axially symmetric flows.

_____

[*]Although α and β are not arbitrary constants but depend on the solution about which linearization is performed, locally the stability limit imposed by Eq. (4.3) may be relaxed for the condition given by Eq. (6.11). In practical applications, however, the difference is unimportant and Eq. (4.3) may be used.

Table 1

$r = |\sigma|_{max} \frac{\Delta t}{\Delta}$	Condition
.65	unstable at 90 cycles (negative densities)
.55	negative velocities at 350 cycles near stagnation point
.45	negative velocities at 640 cycles near stagnation point
.35	no negative densities or velocities at 2500 cycles.

The fact that the velocities became negative for some values
of r, is in itself not an instability. The solution in the
region of the stagnation point did start to diverge from
the known solution when negative velocities were observed.
As the computation proceeded the situation became worse
since the negative values of the x component of velocity
propagated into the mesh away from the stagnation point.
At this point the calculation for the case was terminated.

7. Numerical results

The results of two calculations are presented. The difference scheme (5.5), which includes the artificial viscosity (5.1), was used to obtain these results. The coefficient κ in Eq. (5.3a) was initially set equal to 2 but during the course of the calculation it was reduced to 1. The free stream Mach number is 4.3 and γ, the ratio of specific heats is 1.4. The flow was started impulsively by using the free stream conditions as initial data. In Figure 4 we plot stagnation density vs. number of cycles. Beyond the 2,340-th cycle the values of density everywhere in the flow field are constant to four figures; clearly the method converges. The accuracy in the calculation of the stagnation density is exceptionally good while the error of .96% in the computed stagnation pressure is consistent for the method. Figure 5 shows the density for values of y as a function of x. The distance y has been normalized by the radius of the body. The corner of the body is at x = 1.28. For y = 1, it is seen that there is a rapid variation of the density corresponding to the corner expansion. For y = 2.2, the density, after the shock, decreases linearly corresponding to the fluid expanding past the body. The complete flow field is shown in Figure 6. Here the position of the shock and sonic line are shown with respect to the body. The dashed curve represents the sonic line computed with

the scheme of Lax given in 1952.

(7.1) $w(t + \Delta t) = w(t) + \lambda(D_x w + D_y w) + (D_x^2 w + D_y^2 w)$.

Equation (7.1) is a first order method and the point of
attachment of the sonic line to the body is greater than
3 space increments from the body corner. On the other
hand the high order scheme, Eq. (5.5), gives the position
of the sonic line correctly i.e. within a fraction of one
mesh point of the corner.

As shown in Figure 7, the Mach number at the corner
is 0.975. One mesh point to the right on top of the body
the Mach number is 2.04 while it is 0.666 one mesh point
below the corner, on the body face. Beyond the corner
the Mach number increases very rapidly, indicating a strong
rarefaction wave.

Thus the difference scheme is able to handle such
rapid variations of the flow quantities; this is again
indicated by the distribution of pressure ratio along
the body given in Figure 8. In Figure 9 the entropy
distribution along the stagnation streamline is shown.
The theoretical value of entropy at the stagnation point
can be calculated exactly; it is 2.24 while the computed
value is 2.20. The abrupt entropy change near the
corner and the oscillation on top of the body are very
likely due to the fact that the vertical component of
velocity was computed on the top of the body rather than

prescribed to be zero. This was done so as to observe the number of space steps needed to approach the correct value. This meant that improper values of entropy, mass, etc., were introduced into the flow because of false boundary conditions. The entropy distribution Δ above the body is shown and it approaches the theoretical correct value. The sharp rise in the value of the entropy at the corner is presumably due to the artificial viscosity acting on the steep rarefaction gradients at the corner. In order to resolve this problem, additional work is necessary. Figures 10 and 11 show some results for the case where $M = 10$ and $\gamma = 1.17$. In this calculation it was found necessary to introduce the function

$$\kappa = \kappa_0 \{1 + \exp{(1 - |\vec{u}|/\kappa_1)}\} \quad \text{if } |\vec{u}|/\kappa_1 \leq 1,$$

or

$$\kappa = 1 \qquad \qquad \text{otherwise;}$$

for the coefficient of viscosity given in Eqs. (5.3a). κ_1 was chosen to be of the order of the velocity behind the strong normal shock, while κ_0 was between one half and one; $|\vec{u}|$ is the magnitude of the velocity. This has the effect of providing additional damping near the stagnation point. This damping was not required for the previous case ($M = 4.3$) since the shock was well away from the body. It is felt, for the case $M = 10$, that if unequal spacing were chosen in the x direction, so that there would be more steps between the shock and the body, additional damping would be unnecessary.

Bibliography

[1] Samuel Z. Burstein, Numerical Methods in Multi-
     dimensional Shocked Flow, A.I.A.A. Journal, Vol. 2,
     December 1964, pp. 211-217.

[2] Peter D. Lax and Burton Wendroff, Difference Schemes
     for Hyperbolic Equations with High Order Accuracy,
     Comm. Pure and Appl. Math., Vol. 17, 1964, pp. 381-
     398.

[3] Peter D. Lax and Burton Wendroff, System of
     Conservation Laws, Comm. Pure and Appl. Math.,
     Vol. 13, 1960, pp. 217-237.

[4] Robert Richtmyer, A Survey of Difference Methods
     for Non-Steady Gas Dynamics, NCAR Technical Note
     63-2.

[5] Robert Richtmyer, Difference Methods for Initial-Value
     Problems, Interscience, 1957.

[6] H. U. Thommen and L. D'Attore, Calculation of Three
     Dimensional Supersonic Flow Fields by a Finite
     Difference Method, General Dynamics/Astronautics,
     GDA-ERR-AN539, September 1964.

[7] R. D. Richtmyer and K. W. Morton, Stability Studies
     for Difference Equations, NYO 1840-5, August 25, 1964.
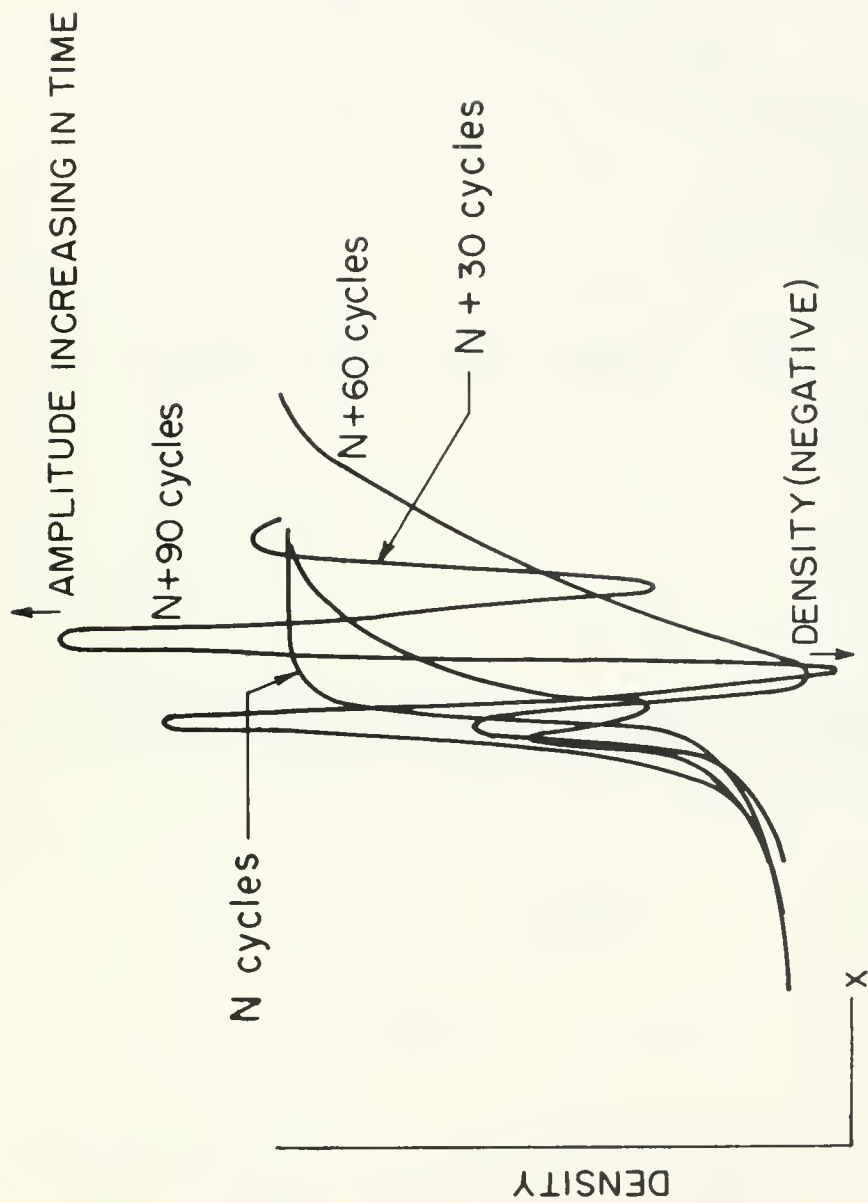
Schematic of Instability Occuring Within the Shockwave
for Modified Lax-Wendroff Scheme

Figure 2

420
350
280
210
140
70
0

SONIC LINE N= 420 CYCLES
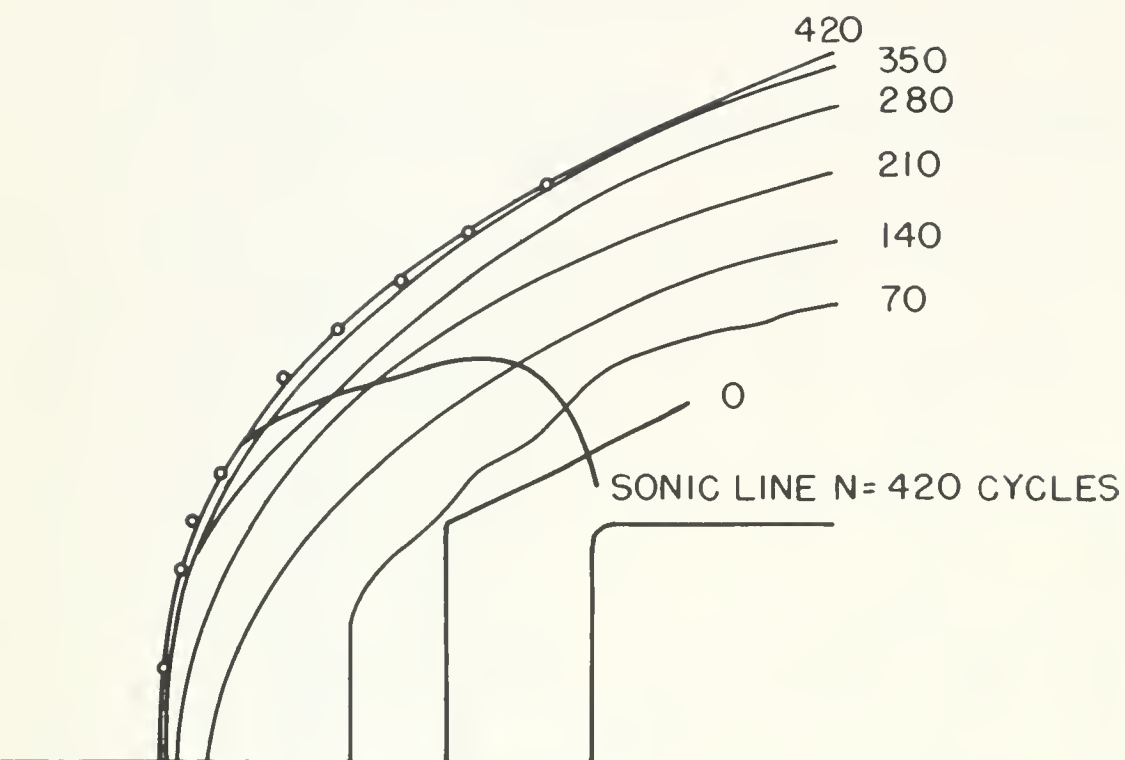
Time Dependent Solution Showing Shock Position for Modified Lax-Wendroff Scheme. Numbers Refer to Computational Cycles.

Figure 3
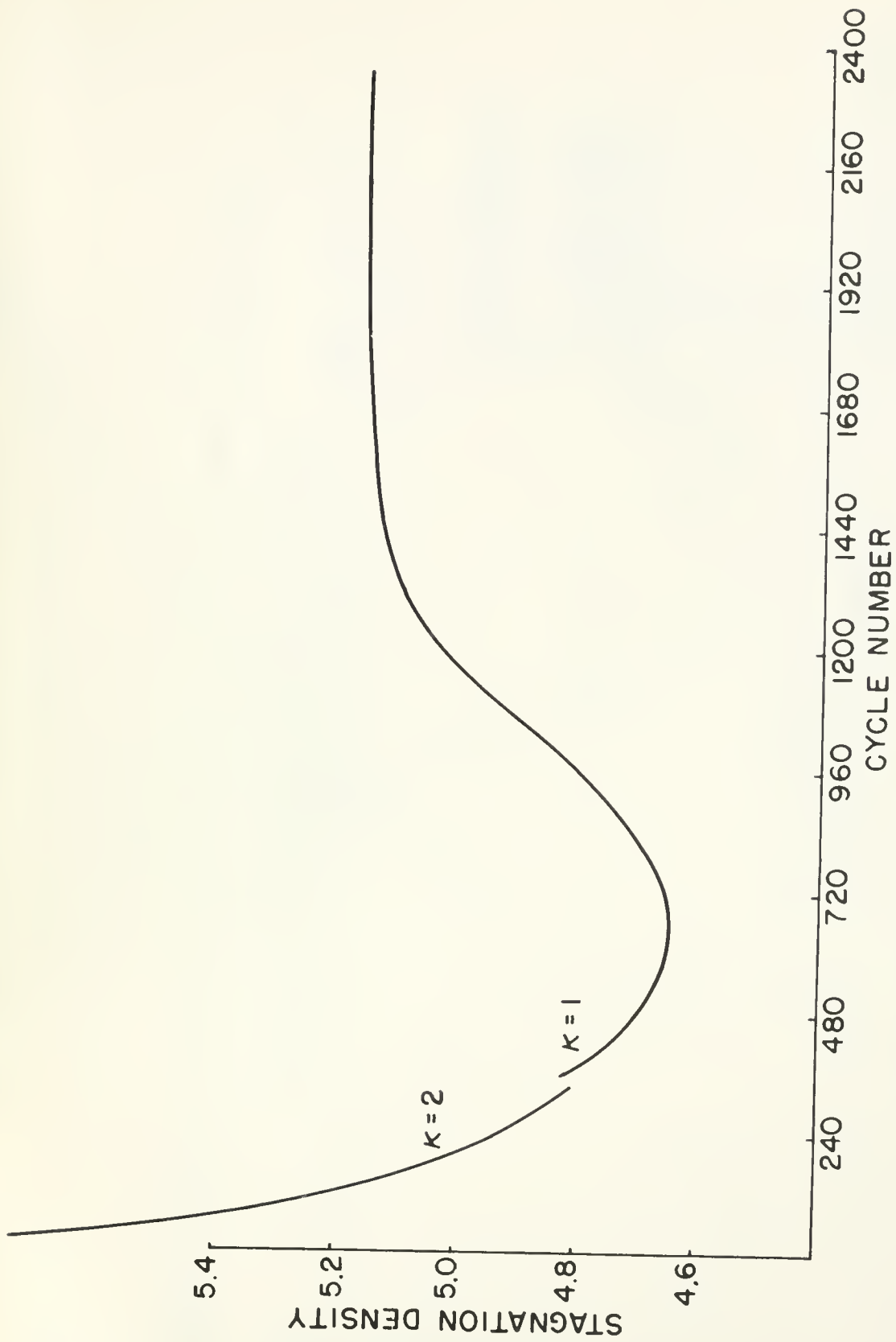
Convergence of Time Dependent Solution, Stagnation Density (M = 4.3, γ = 1.4)
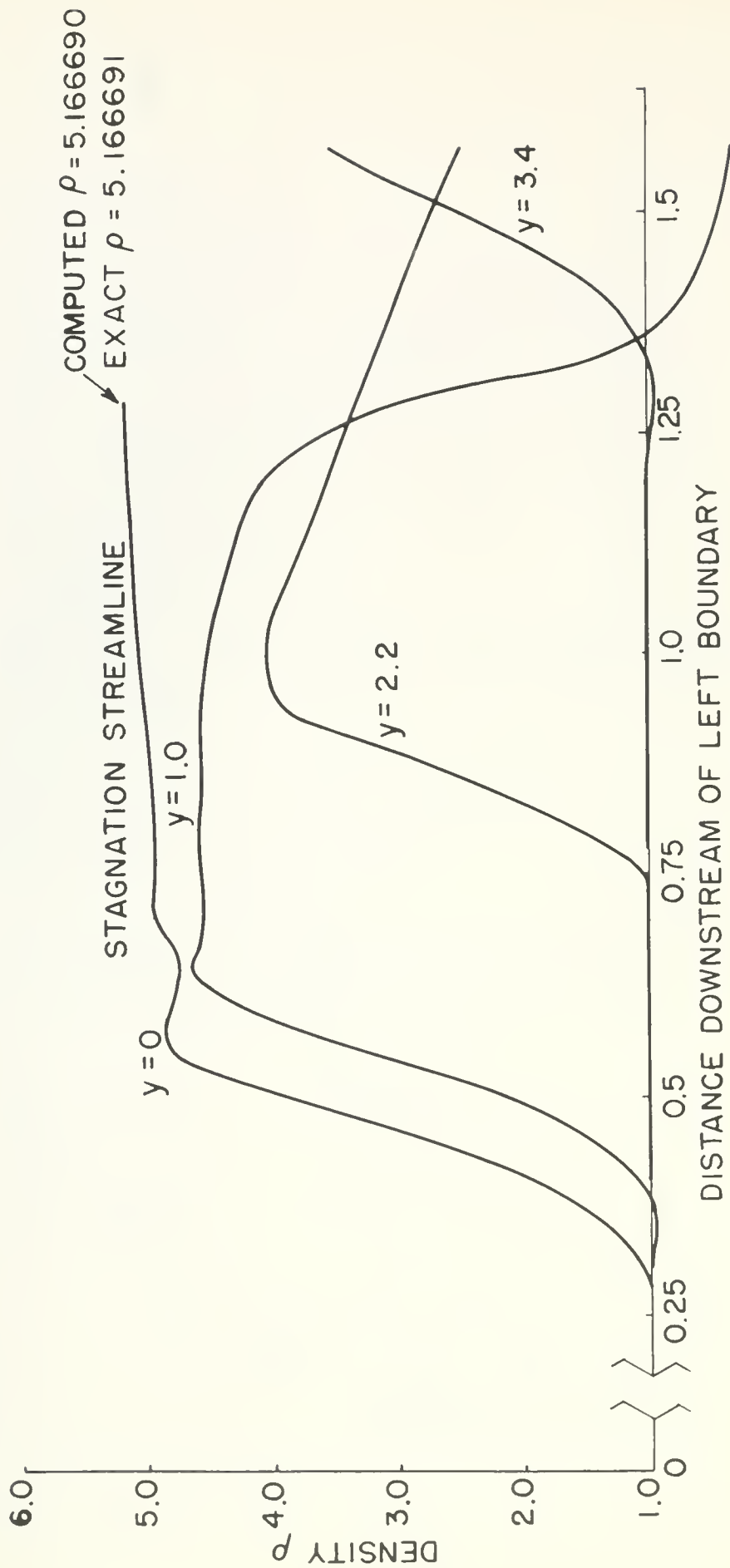
Figure 4

Density Distribution Along Some Coordinates y = Constant, Normalized with Body Radius, M = 4.3, γ = 1.4

Figure 5

SONIC LINE
EQUATION (5.5)

SONIC LINE
EQUATION (7.1)
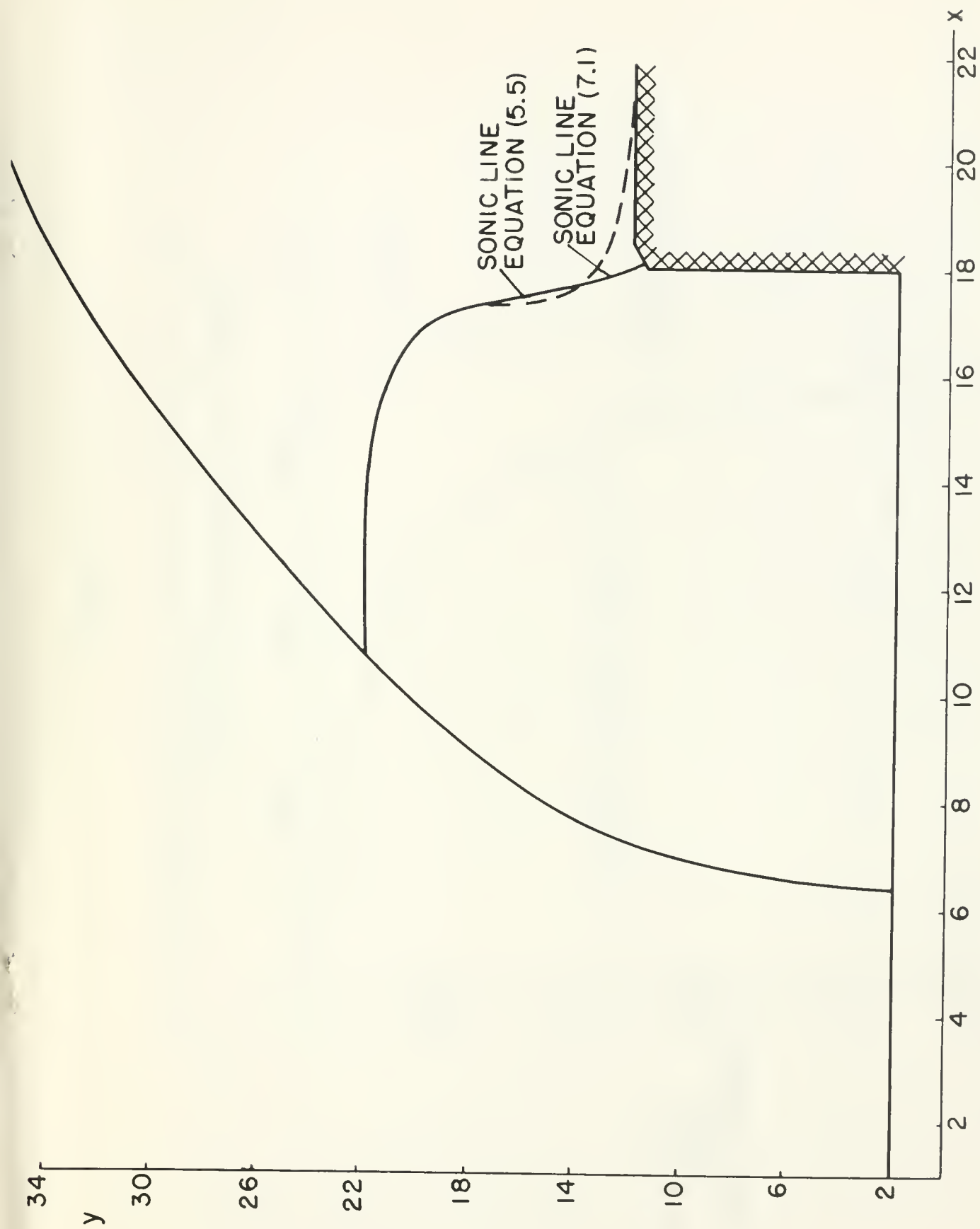
Flow Field Showing Detached Shock and Sonic Line for M= 4.3, γ=1.4 , Detachment Distance = 1.16

Figure 6
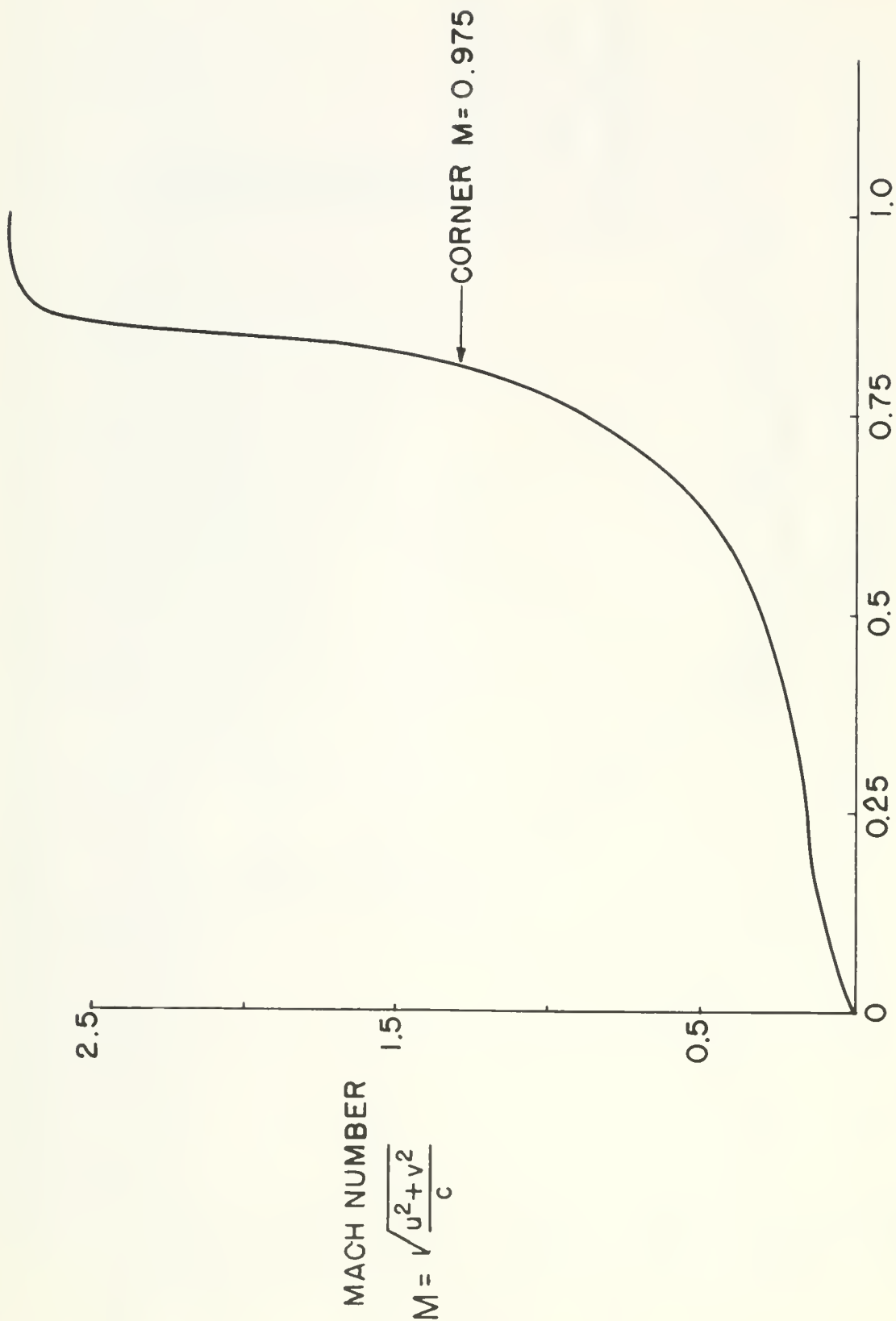
Mach Number Distribution Along Blunt Body, M = 4.3, $\gamma = 1.4$

Figure 7
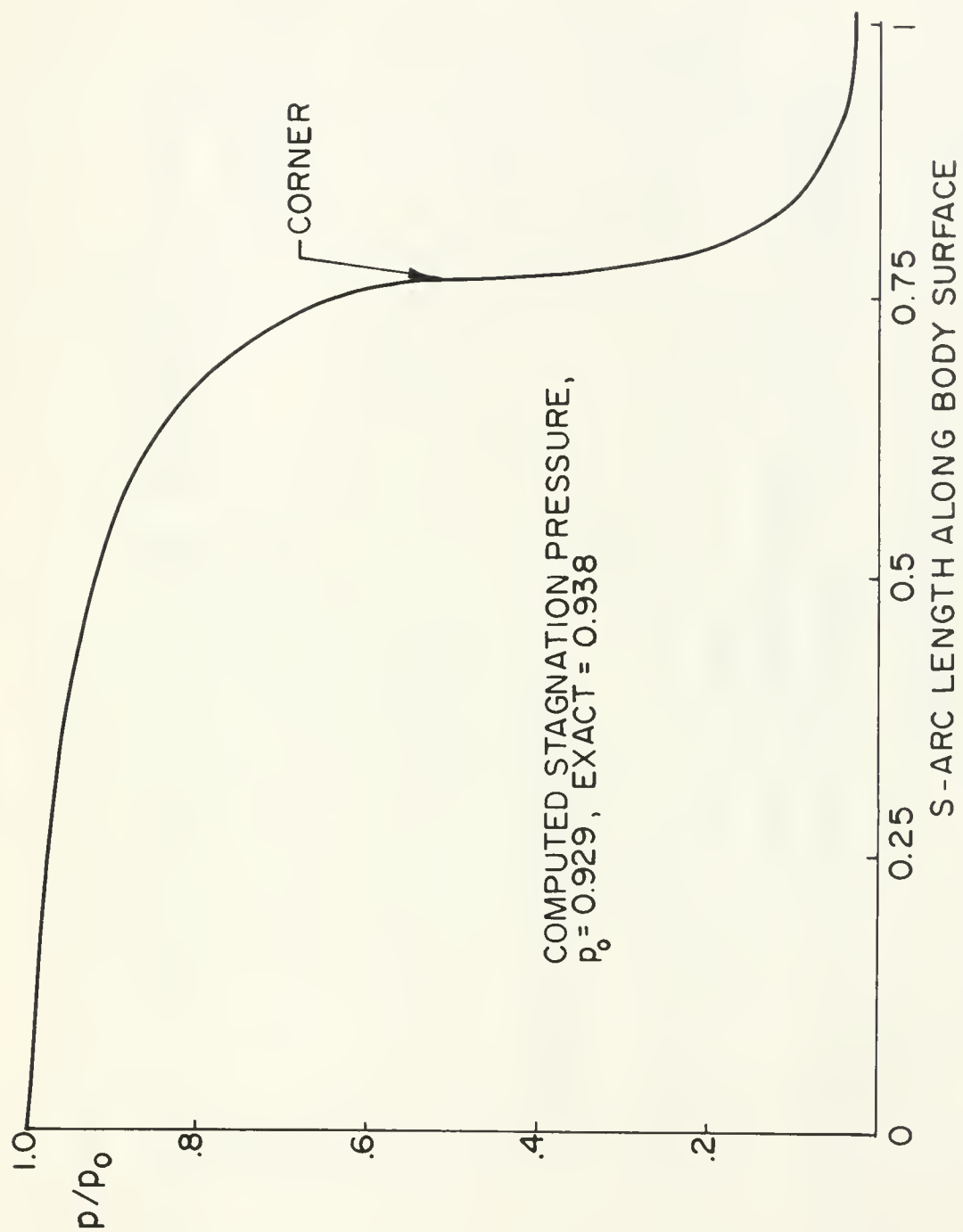
Pressure Ratio Along Blunt Body, M = 4.3, γ = 1.4
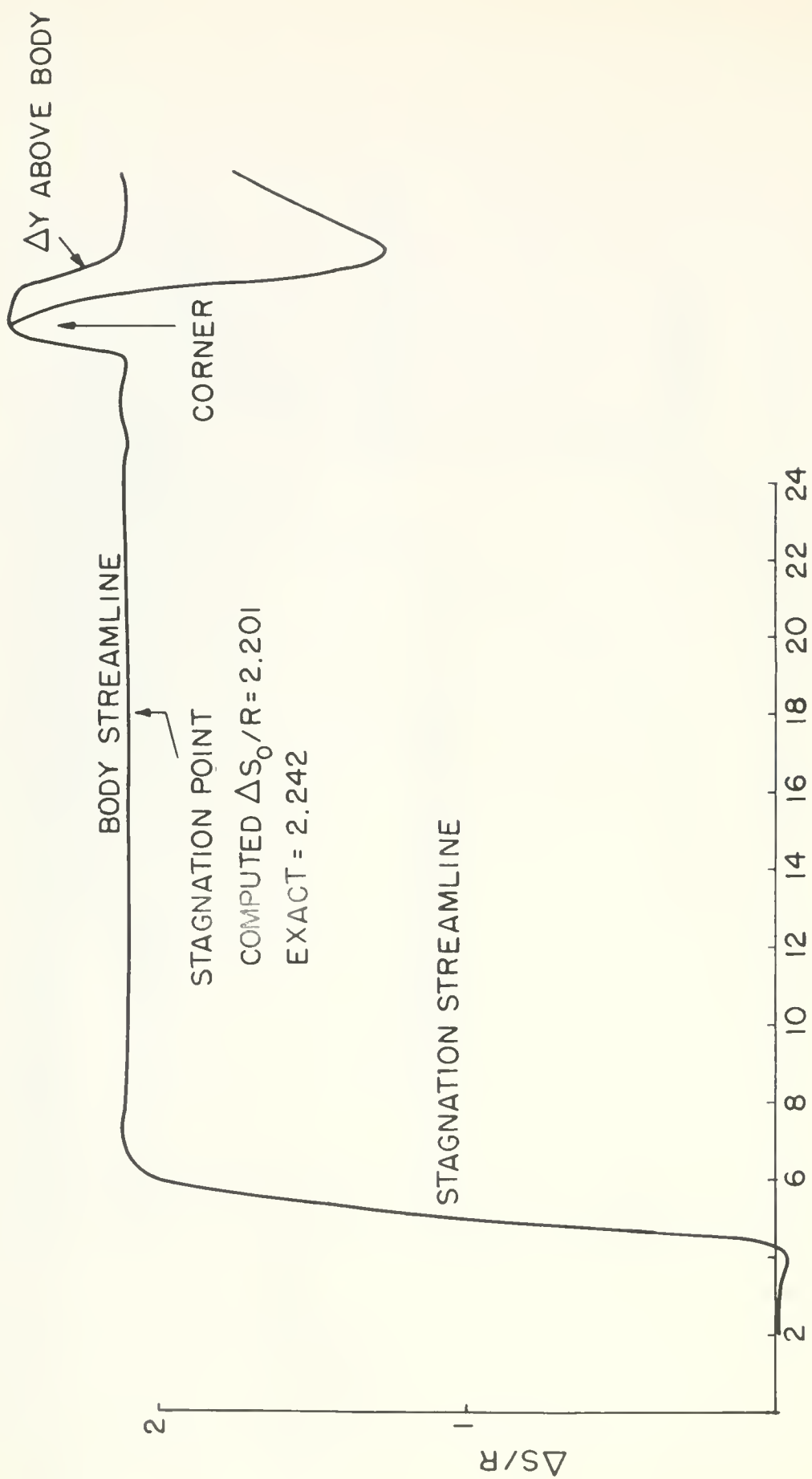
Figure 8

Entropy Distribution Along Stagnation Streamline and Body Streamline

Figure 9

Density Distribution Along Some Coordinates y = Constant, Normalized with Body Radius
M = 10, γ = 1.17
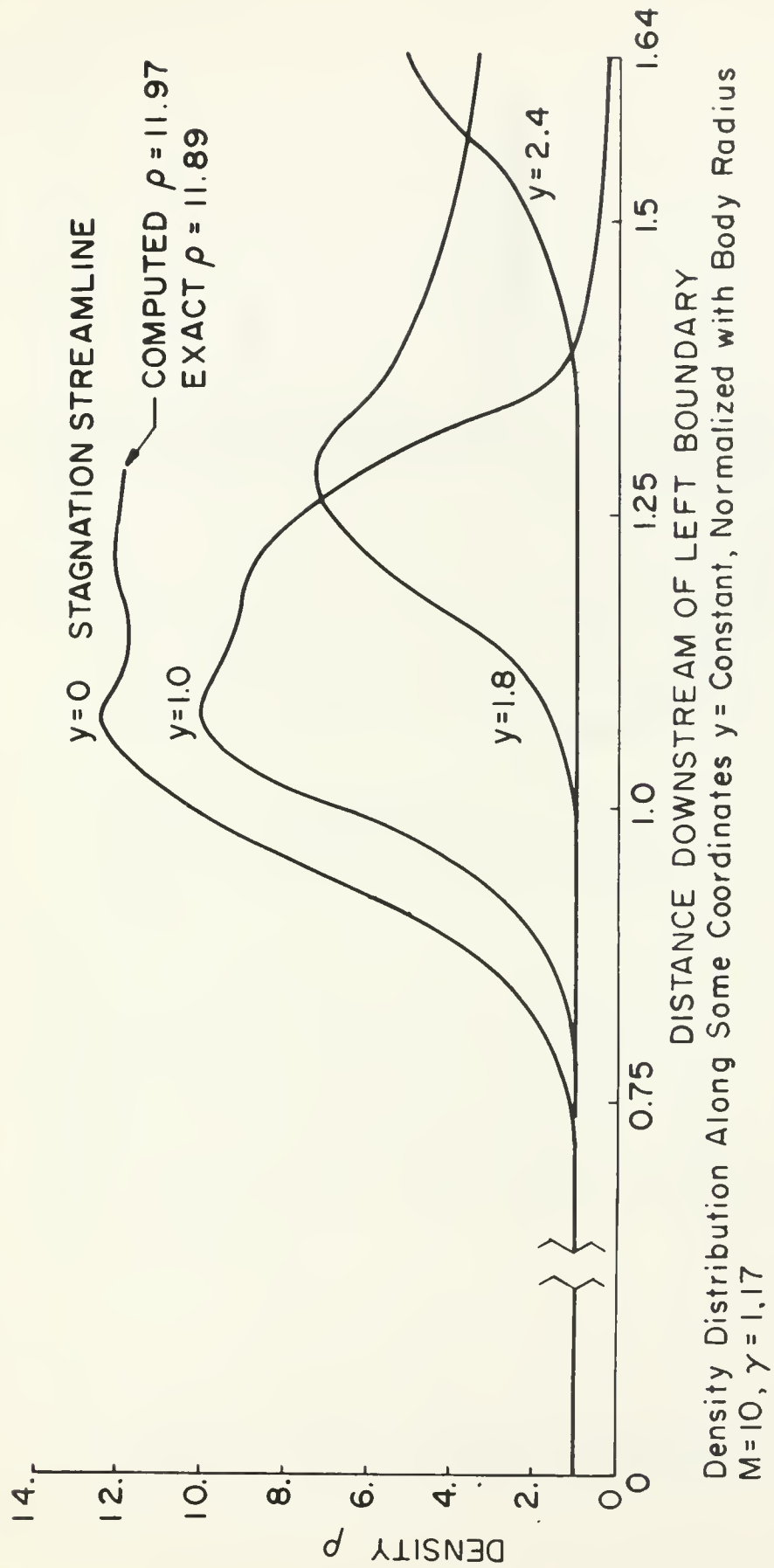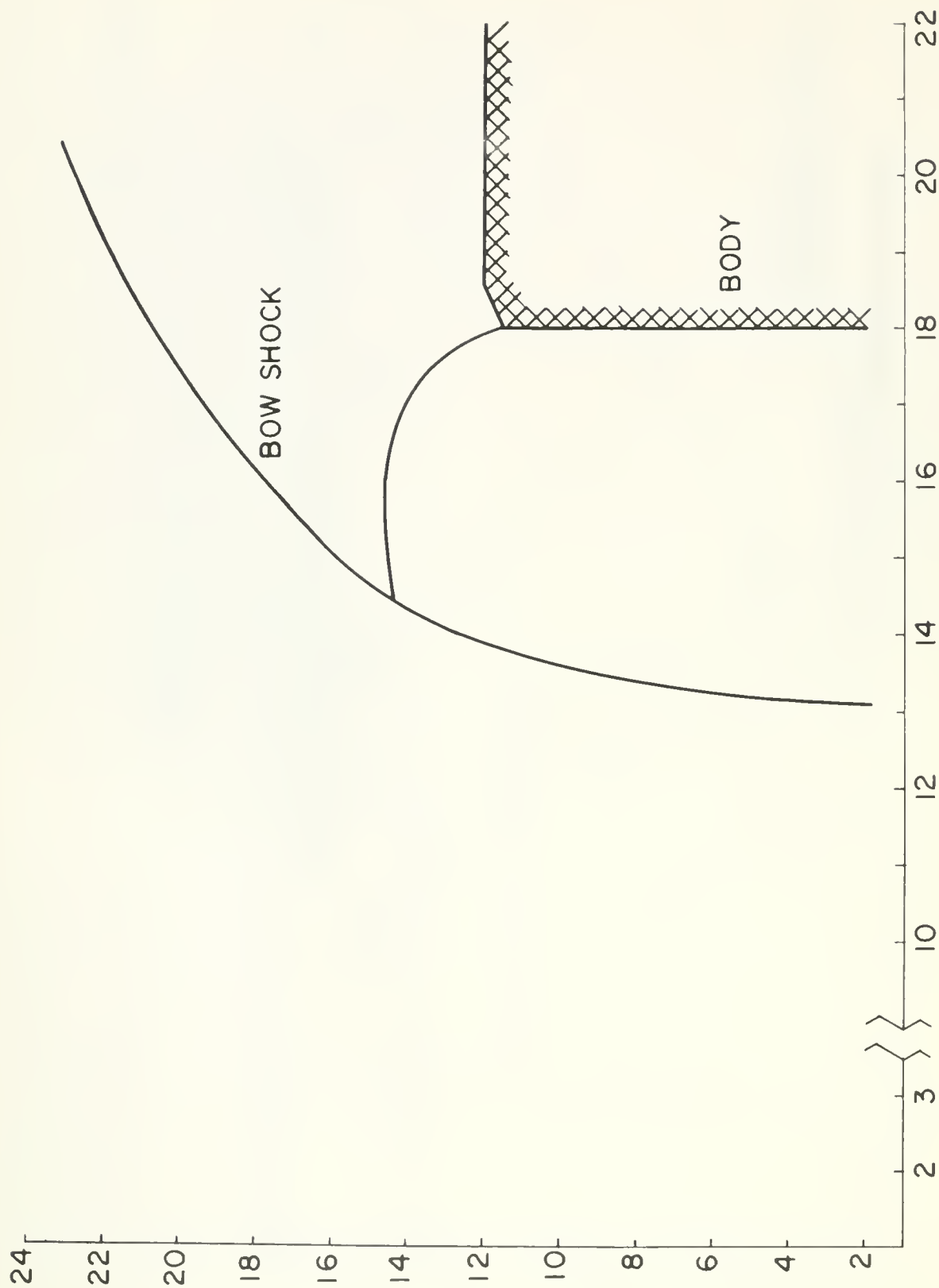
Figure 10

Flow Field Showing Detached Shock and Sonic Line for M=10, γ=1.17, Detachment Distance = 0.49

Figure 11